BBA - Bioenergetics 1860 (2019) 689–698

Contents lists available at ScienceDirect

BBA - Bioenergetics

journal homepage: www.elsevier.com/locate/bbabio

Binding of ferredoxin NADP$^+$ oxidoreductase (FNR) to plant photosystem I

Pini Marco, Tamar Elman, Iftach Yacoby*

School of Plant Sciences and Food Security, The George S. Wise Faculty of Life Sciences, Tel Aviv University, Ramat Aviv, Tel Aviv 69978, Israel

ARTICLE INFO

Keywords:
PSI
FNR
Binding
ITC
Photosynthesis
Membrane

ABSTRACT

The binding of FNR to PSI has been postulated long ago, however, a clear evidence is still missing. In this work, using isothermal titration calorimetry (ITC), we found that FNR binds to photosystem I with its light harvesting complex I (PSI-LHCI) from *C. reinhardtii* with a 1:1 stoichiometry, a Kd of ~0.8 μM and ΔH of −20.7 kcal/mol. Titrations at different temperatures were used to determine the heat capacity change, ΔCP, of the binding, through which the size of the interface area between the proteins was assessed as ~3000 Å^2. In a different set of ITC experiments, introduction of various sucrose concentrations was used to estimate that ~95 water molecules are released to the solvent. These observations support the notion of a binding site shared by few of the photosystem I - light harvesting complex I (PSI-LHCI) subunits in addition to PsaE. Based on these results, a hypothetical model was built for the binding site of FNR at PSI, using known crystallographic structures of: cyanobacterial PSI in complex with ferredoxin (Fd), plant PSI-LHCI and Fd:FNR complex from cyanobacteria. FNR binding site location is proposed to be at the foot of the stromal ridge and above the inner LHCI belt. It is expected to form contacts with PsaE, PsaB, PsaF and at least one of the LHCI. In addition, a ~4.5-fold increased affinity between FNR and PSI-LHCI under crowded 1 M sucrose environment led us to conclude that in *C. reinhardtii* FNR also functions as a subunit of PSI-LHCI.

1. Introduction

Oxygenic photosynthesis takes place in the chloroplast of cyanobacteria, green algae and higher plants. Through this process, light energy is transformed into chemical energy in the form of electrons passing through the different components of the thylakoid membrane. This energy is stored by the synthesis of two molecules, NADPH and ATP, which are used to assimilate inorganic carbon through the Calvin-Benson-Bassham cycle. The capture of light energy and electron transfer take place in the thylakoids membrane – a dynamic landscape where large membrane-spanning protein complexes, such as photosystem I (PSI), interact with smaller proteins. PSI is an extremely efficient photoelectric apparatus, exhibiting a quantum efficiency of almost 100% [1]. The ability of PSI to convert sunlight energy to chemical energy is highly dependent on the precise spatial arrangement of the protein subunits and light harvesting complexes (LHC) as well as the relative positions of its cofactors, *e.g.* the Iron–sulfur (FeS) redox clusters FX, FA and FB. In addition, proper interaction of PSI with external proteins such as plastocyanin (Pc) and ferredoxin (Fd) is a prerequisite for efficient electron transfer. Among these proteins, Fd is a soluble electron acceptor, reduced by PSI and located in the stromal area of the chloroplast [2]. Fd functions as an electron mediator, which distributes reducing equivalents from PSI to downstream sinks [3]. The primary sink for reduced Fd is ferredoxin-NADP+ reductase (FNR), which generates NADPH [4,5].

1.1. The interactions of FNR and the thylakoid membrane

The interaction of FNR with the thylakoid membrane has been subject to many studies in the last three decades, since it is considered as a potential mechanism to define the fate of photosynthetically derived electrons [6]. Early studies suggest that FNR is tightly associated with the membrane [7,8] and that its binding to the membrane determines its activity [9,10]. According to a study in spinach chloroplasts, FNR is functional in its soluble form and approximately 50% of its pool is not membrane bound [11]. Studies in spinach leaves coupled the association of FNR to the membrane *via* a 17.5 kDa protein (or 10 kDa as in [12]) that was named connectein [13,14]. Although the exact identification of connectein was never fully disclosed in the thylakoid membrane, it shares high similarity with the 16.5 kDa PsbQ(like) protein of the oxygen evolving complex in the thylakoid's lumenal side [15]. This complex consists of two FNRs and one connectein. Nevertheless, FNR can also bind the thylakoid membrane in the absence of connectein [14].

* Corresponding author.
E-mail address: iftachy@tauex.tau.ac.il (I. Yacoby).

https://doi.org/10.1016/j.bbabio.2019.07.007
Received 2 April 2019; Received in revised form 11 July 2019; Accepted 18 July 2019
Available online 20 July 2019
0005-2728/ © 2019 Elsevier B.V. All rights reserved.

In spinach, an interaction of FNR with the Cytochrome (Cyt) *b6f* complex has also been observed and described as "firm binding" [16], only to later be questioned by the same group [17]. Furthermore, a determined stoichiometry of 0.9 FNR molecules per Cyt *b6f* monomer and tight association in general ruled out the possibility of an artifact [11]. Cyt *b6f* activity was not affected in the absence of FNR; however, *in vitro* reduction of the Cyt *b6f* haem *b*H by NADPH was mediated by bound FNR and required Fd presence [11,18], thus suggesting a possible role of FNR in Fd-dependent route of cyclic electron transfer [19–21].

The thylakoid membrane embedded NAD(P)H dehydrogenase (NDH) complex has a key function in) another pathway of (cyclic electron transfer around PSI. Association of the NDH complex with FNR was previously reported [20–22], pointing to an involvement of FNR as a diaphorase, extracting electrons from NADPH and delivering them through Fd to the NDH complex and plastoquinone (PQ) pool [23]. In further support of this, a super-complex of PSI and NDH from plant was recently shown [23,24].

A few more proteins anchoring FNR to the thylakoid membrane were identified in recent years. One of them is Tic62, a subunit of the Tic complex (a translocon in the inner envelope of chloroplasts) that is also present in the thylakoids of plants [25]. Tic62 was shown to be tightly associated with the leaf FNR isoform, yet this complex does not co-migrate with PSI, Cyt *b6f* or NDH complexes [25]. In a *tic62* mutant strain the thylakoid-localized pool of FNR was reduced by about 50% while the soluble FNR pool remained the same, pointing to the important role of Tic62 in keeping FNR attached to the membrane. In addition, the amount of Tic62:FNR complexes decreased markedly upon illumination or at alkalized pH. This led to the suggestion that the Tic62-dependent bound FNR serves a purpose in sensing and regulation of the redox state [25]. Alternatively, it was proposed that by complexing with Tic62, FNR is somehow protected from inactivation during photosynthetic idleness in the dark [21,25]. Another FNR anchor is TROL (thylakoid rhodanase-like). This transmembrane protein exhibits an FNR association pattern [26], which is similar to that of Tic62. On the basis of the light/pH dependent dissociation of FNR:Tic62/TROL complexes, it was suggested that stabilization of FNR at the membrane during dark periods minimize NADPH oxidation by FNR [25]. It should be noted that in *C. reinhardtii* there are no known orthologues of Tic62 and TROL [6], thus any function of Tic62/TROL-dependent FNR recruitment to the thylakoid membrane would possibly be fulfilled by some different component(s).

PSI was also shown as a binding partner of FNR at the thylakoid membrane. Andersen et al. (1992) isolated FNR:PSI complexes from barley with a stoichiometry of 0.4 ± 0.2 FNR molecules per PSI [27]. The bound FNR was capable of NADP+ photo-reduction, though the mean rate for the reaction was ~6 times higher when a saturating amount of FNR was added. Cross-linking and western blotting experiments revealed that the bound FNR interacts with PsaE [27]. In a different study, Weber and Strotmann (1993) have shown that, in spinach thylakoids, PsaE was more sensitive towards the chaotropic agent NaSCN than FNR and was released from the membrane at lower salt concentrations [28]. This observation led to the conclusion that PsaE is not the main anchor for FNR in thylakoids [28]. Nevertheless, since anti-PsaE antibody inhibited NADP+ reduction in their experiments. The authors explained it as a possible sterical hindrance by the antibody in the vicinity of PsaE, likely inhibiting the approach of Fd to PsaE-bound FNR [28]. Following this work, van Thor et al. (1999) demonstrated dependence of NADP+ photo-reduction activities on PsaE in PsaE-deficient membranes of *Synechocystis* [29]. This work was contradicted by Cassan et al. (2005), who compared the kinetics of reduced Fd re-oxidation by FNR and NADP+ between wild type and PsaE-less PSI particles from *Synechocystis* [30]. Due to the very similar kinetics for both PSIs, it was determined that the PsaE subunit is not involved in NADP+ reduction [30]. However, it was speculated in an earlier study that PsaE plays a different role between higher plants and cyanobacteria based on an exposed N′ terminal region of PsaE in spinach while both N′ and C′ termini were found to be buried in *Synechocystis* PSI [31]. In summary, notwithstanding the conflicting studies, it seems that PsaE role in recruiting FNR to the stromal ridge of PSI is well based.

More support for the association of FNR with the various thylakoid membrane components comes from recent studies in *C. reinhardtii*, where FNR has been reported to be part of a state II super-complex and/or a putative CEF super-complex. Iwai et al. (2010) as well as Mosebach et al. (2017) reported the isolation of a PSI-LHCI-LHCII-Cyt *b6f*-FNR-PGRL1 super-complex [6,18], and Takahashi et al. (2013) showed that this super-complex can be isolated in state I conditions, *i.e.* in the absence of LHCII [32]. A Cyt *b6f*/PSI ratio of 1:1 was determined, but precise stoichiometry values for the other components were missing [18]. The reduction of Cyt *b* by NADPH in the presence of Fd implies that FNR was bound to Cyt *b6f* in the super-complex [18]. However, it cannot be determined whether FNR was also bound to PSI in that potential CEF super-complex. In a later work by Takahashi et al. (2014), a PSI-LHCI-LHCII-FNR super-complex was isolated from state II cells, strongly indicating a direct binding between FNR and PSI [33]. It was supported in a more recent work by Bergner et al. (2015), in which PSI-LHCI-FNR-LHCSR3 super-complex was isolated from state I thylakoids using a *stt7* mutant strain [34]. The immunoblot of the super-complex showed a strong Cyt *f* signal, however, the signal peaked in a different fraction (of the different sucrose gradient fractions) and so the authors did not include Cyt *b6f* as part of the complex [34]. Recently, a complex between PSI and Cyt *b6f* was isolated from *Arabidopsis* thylakoid membranes and observed by electron microscopy [24]. It is interesting to note that the Cyt *b6f* binding site was located next to the peripheral antennae subunit Lhca1; together with the adjacent Lhca4 subunit (Lhca1 and Lhca8 in *C. reinhardtii*, respectively [35]) this subunit is in close proximity to the PsaE subunit where FNR was reported to form contacts [27].

1.2. Isothermal titration calorimetry

Isothermal titration calorimetry (ITC) is a technique for studying protein–protein interactions that directly measures the thermodynamic parameters of the binding events. In a typical experiment, the net change in heat released or absorbed by the system is recorded along a titration of a given macromolecule with its ligand. The dissociation constant (Kd), binding enthalpy (ΔH) and stoichiometry (N) are measured simultaneously in a single experiment [36–38]. Binding affinities of a few nM can be measured using ITC, obviating the need for labeling. However, large amounts of homogenous, stable and active binding partners are required [39,40]. These requirements, together with the general heat sensitivity of membrane proteins, are challenging and limit studies with membrane proteins using ITC [40]. Indeed, to our knowledge there are only few publications examining the binding properties of photosynthetic proteins using ITC. For example, the binding of several herbicides to photosystem II was assessed using ITC [41]. Data from several studies exists for the interaction between Fd and FNR [37,42,43]. PsaD from cyanobacteria was expressed in *E. coli* and its binding to PsaD-less PSI was assessed by ITC, resulting in a Kd of ~130 nM [44]. Most relevantly, Fd binding to heterologously expressed PsaD yielded a Kd of ~50 nM [45]. Recently, using ITC, we studied the associations of PSI*, an immature form of the complex [46,47], and PSI-LHCI with Fd from *C. reinhardtii*; it was shown that PSI-LHCI has a single binding site for Fd, but the association consists of two distinct binding events, each with a specific affinity [46]. The obtained affinity values, Kd in the range of 0.03–0.3 μM, reflect a tighter binding than that of PSI* and that reported in the past for the algae (6–9 μM) [48–50].

In this work, we seek to elucidate some of the mystery regarding the interactions of PSI with FNR. FNR's location in close proximity to the Fd active site is surely no coincidence, yet little attention has been paid to

the role of its binding to PSI. To do so requires analysis of the arrangement of components involved in electron mediation and reduction at the stromal part of PSI. Therefore, we have performed a thorough ITC study of FNR binding to two active sub-populations of PSI (mature and immature) isolated from the model organism *C. reinhardtii*.

2. Materials and methods

2.1. Expression and purification of recombinant proteins

FNR was heterologously expressed in *E. coli* BL21 cells as described in [46]. The *C. reinhardtii* gene FNR was cloned into pET21b vector as a fusion to maltose binding protein (MBP) with a His6-tag, separated by a linker (3xGGGGS) and TEV protease cleavage site (TEVc). His6:MBP:-TEVc:FNR *E. coli* culture was grown in TB medium and induced by 50 μM isopropyl β-D-1-thiogalactopyranoside (IPTG, Formedium). Following expression, the fusion protein was loaded on a HisTrap HP Ni2+ column (GE Healthcare) and eluted with 500 mM imidazole (Sigma-Aldrich). Cleavage was performed by the addition of a 1:20 (w/w) amount of TEV protease (60 min, 34 °C; described in [46]). Then imidazole was removed using a desalting column (Centri Pure P25, emp Biotech). Cleaved FNR protein was flowed again through a HisTrap column; the column's flow through was collected as the product while MBP with His tag remained bound to the Ni column. Gel filtration chromatography (HiLoad 16/600 Superdex 200 prep grade column, GE Healthcare) was performed to separate the FNR from remaining TEV protease. FNR concentrations were determined spectrophotometrically according to the extinction coefficients $\Sigma 458\,nm = 10{,}700\,M^{-1}\,cm^{-1}$ for FNR [51].

2.2. Algae growth and thylakoids preparations

PSI-LHCI was purified from thylakoid membranes of *C. reinhardtii* strain JVD-1B[pGG1] [52] as described in [46]. Chlorophyll (Chl) concentration was determined spectrophotometrically after extraction in 90% acetone according to [53].

2.3. Isolation of PSI

PSI purification followed the protocols described in [52,54]. Thylakoids were diluted to 0.8 mg Chl/ml in solubilization buffer: 25 mM Hepes-KOH, 100 mM NaCl, 5 mM MgSO4, 10% glycerol (pH 7.5), solubilized by the addition of 1/10 volume of 10% n-Dodecyl β-D-maltoside (DDM; Anatrace Inc.) and then gently mixed in the dark (30 min, 4 °C). Following centrifugation (46,000*g*, 25 min, 4 °C) the supernatant was loaded onto a HisTrap HP Ni2+ column pre-equilibrated with solubilization buffer +0.03% DDM and washed with the same buffer supplemented with 2 mM imidazole until UV absorbance reached a baseline. PSI was eluted by 1 column volume of 25 mM MES-NaOH, 100 mM NaCl, 5 mM MgSO4, 10% glycerol, 0.03% DDM, 300 mM imidazole (pH 7.0) buffer. The eluted PSI was loaded on sucrose density gradient tubes [54] made by freezing and thawing 0.65 M sucrose in 20 mM Tricine-NaOH, 0.03% DDM (pH 7.7) buffer and separated by centrifugation (160,000*g*, 24 h, 4 °C).

2.4. Determination of P700 concentration of the isolated PSI

An amount of PSI corresponding to 40 μg Chl was solubilized in 1 ml of 20 mM Tricine-NaOH, 10 mM ascorbate, 100 nM 2,6-dichlorophenol indophenol (DCPIP; Sigma-Aldrich), 10 nM Pc (pH 7.7) buffer, and placed in a quartz cuvette. By projecting the cuvette with saturating white light (Intralux 5000, Volapi) the reduced minus oxidized absorption difference in 700 nm (ΔA700nm) was recorded spectrophotometrically (Cary 50, Varian). The particles were re-reduced in the dark and photo-oxidized several more times ($n = 9$); the mean ΔA700nm was calculated. P700 (which corresponds to the reaction center of PSI) concentrations were determined by using an extinction coefficient of $100{,}000\,M^{-1}\,cm^{-1}$ [55].

2.5. Isothermal titration calorimetry (ITC)

2.5.1. Theory

The relation between the Gibbs free energy of the interaction, ΔG, and the dissociation constant, Kd is given by:

$$\Delta G = RT\ ln\ Kd \tag{1}$$

The contribution of the entropy of binding, ΔS, to the Gibbs free energy is calculated according to:

$$\Delta G = \Delta H - T\Delta S \tag{2}$$

where ΔG, ΔH and ΔS are measured in kcal/mol and Kd is measured in M. -TΔS describes the entropy component of the binding.

Exchange of protons between ionizable groups in any of the binding partners and the bulk solvent results in a contribution to the measured binding enthalpy change from ionization of the buffer [43,56] according to:

$$\Delta H = \Delta H^0 + n_{H+}\Delta H_{ionization} \tag{3}$$

where ΔH0 is the buffer-independent binding enthalpy and nH+ is the net number of protons exchanged between the complex and the solvent. ΔHionization is the intrinsic buffer ionization enthalpy.

By performing a given binding assay at variable temperatures, one can estimate the heat capacity change of the binding, ΔCP, according to [43]:

$$\Delta C_P = \left(\frac{\partial \Delta H}{\partial T}\right) \tag{4}$$

where ΔCP is measured in cal $K^{-1}\,mol^{-1}$.

The relation between the heat capacity change associated with structural changes such as protein un-folding and protein-protein interactions is given by the following equation:

$$\Delta C_P = 0.45\ \Delta ASA_{apolar} - 0.26\ \Delta ASA_{polar} + 0.17\ \Delta ASA_{OH} \tag{5}$$

where ΔASAapolar and ΔASApolar are the change in accessible solvent area of the buried protein's apolar groups and polar groups, respectively [57–59]. ΔASA_{OH} is the change derived from Ser and Thr hydroxyl groups [60]. ΔASA is measured in Å2, and the relation between its components and the binding enthalpy at the reference temperature of 60 °C, ΔH(60 °C), is according to the following equation [43,57,59]:

$$\Delta H\,(60°C) = -8.44\ \Delta ASA_{apolar} + 31.4\ \Delta ASA_{polar} \tag{6}$$

where ΔH(60 °C) is the binding enthalpy at the reference temperature of 60 °C, which corresponds to the median temperature at which protein denature. PSI is unstable at much lower temperatures, and thus ΔH (60 °C) couldn't be obtained experimentally. Therefore, the relation in Eq. 4 may be used to calculate ΔH(60 °C) according to [43]:

$$\Delta H_{int}(T) = \Delta H_{int}(T_0) + \Delta C_P(T - T_0) \tag{7}$$

where ΔH_{int} is the intrinsic binding enthalpy at any temperature T (*e.g.* 60 °C) and T_0 is a reference temperature (*e.g.* 25 °C), assuming that the ΔH dependence on the temperature is linear in this range.

Finally, the number of water molecules exchanged between the complex and the bulk solvent during the interaction (nW) can be calculated based on the relation between the binding strength and the buffer osmolality, measured in mol/Kg, using the equation [61,62]:

$$\frac{\partial\, ln\, K_A}{\partial osmolality} = -\frac{n_W}{55.6} \tag{8}$$

where Ka is the binding association constant (1/Kd).

2.5.2. Protocol

PSI and FNR were concentrated by centrifugation (1500*g*, 4 °C) in a

filtering device (Amicon Ultra-15, 50,000 or 10,000 MWCO; Merck-Millipore) to the desired concentrations of 10–20 μM for PSI and 100–200 μM for FNR. Dialysis in a bag was performed in order to effectively match the buffers of PSI and FNR: The proteins were dialyzed (dialysis tubing cellulose membrane 14,000 MWCO, Sigma-Aldrich) overnight against ×200 volume of the experiment buffer, while stirring in the dark in 4 °C. ITC experiments were carried out using the MicroCal PEAQ-ITC (Malvern) in a dark room. FNR, at 70–150 μM concentrations in the syringe, was titrated (12 × 3.2 μl injections) against 5–20 μM PSI in the ITC cell at 25 °C and a stirring speed of 750 rpm. The experiments were performed with either 50 mM Hepes-KOH, 0.05% DDM (pH 7.5) buffer ($n = 4$), 50 mM Tricine-NaOH, 0.05% DDM (pH 7.5) buffer (n = 4) or 25 mM sodium phosphate, 0.05% DDM, (pH 7.5) buffer ($n = 3$). Experiments were also performed in 50 mM Hepes-KOH, 0.05% DDM (pH 7.5) buffer in different temperatures: both at 10 °C (n = 4) and 17 °C (n = 3). A final set of experiments was performed in different osmotic stress conditions, using 50 mM Hepes-KOH, 0.05% DDM (pH 7.5) buffer supplemented with 0.25 M sucrose ($n = 1$), 0.5 M sucrose ($n = 2$) or 1 M sucrose (n = 1). Data were fitted using the 'One Set of Sites' model (PEAQ-ITC Analysis Software).

3. Results

3.1. Studying the FNR binding to PSI-LHCI and PSI* isolated from C. reinhardtii

The binding of FNR to PSI-LHCI was investigated by ITC. Fig. 1 shows a typical experiment, in which FNR was titrated into a sample cell containing PSI-LHCI, at pH 7.5, 25 °C. Each injection of FNR into the cell generated an exothermic heat signal, seen as negative peaks in the raw heat plot (Fig. 1A, bottom). The integrated heat curve (Fig. 1A top) showed a maximum inflection at FNR:PSI-LHCI ratio of ~1.0. Following the recording of the heat changes, the "PEAQ-ITC Analysis Software" was used to fit the data according to the 'One Set of Sites' model. The fit resulted in a mean stoichiometry (N value) of 0.94 ± 0.02, and so the reaction's stoichiometry was determined as 1.0 FNR binding site per PSI-LHCI. The reaction dissociation constant, Kd of 780 ± 110 nM, and the binding enthalpy, ΔH of −20.7 ± 0.8 kcal/mol ($n = 4$), were also determined. The binding free energy change, ΔG, and the entropy change, −TΔS, were calculated as −8.3 kcal/mol and 12.4 kcal/mol, respectively (Eqs. (1)–(2)). Accordingly, the exothermic binding reaction of FNR to PSI-LHCI is driven by the favorable enthalpy component (Fig. 1B).

Titrations performed in varying buffer systems revealed that at pH 7.5 there was no significant buffer dependency of FNR:PSI-LHCI binding enthalpy within the error limits, as can be seen from the nearly invariant values of binding enthalpy. Thus, at pH 7.5 the net number of protons exchanged between the binding partners and the solvent (nH +) appears negligible and ΔH0, the buffer-independent binding enthalpy, may be accounted as the mean ΔH of all the experiments at 25 °C (ΔH0 pH 7.5, 25 °C = −21 ± 1.2 kcal/mol, $n = 11$), according to Eq. (3).

Next, we were interested in gaining further insight as to the area of interaction between FNR and PSI. For that goal, a powerful application of the ITC method can be exploited. By performing a given binding assay at variable temperatures, one can estimate the heat capacity change of the binding (ΔCP). Therefore, FNR:PSI-LHCI binding interaction was examined at different temperatures and the enthalpy change upon binding was shown to decrease linearly with the temperature ($p \leq 0.001$, Fig. 3). Linear regression of the measured ΔH at different temperatures yielded a ΔCP of $-340 \pm 80\ \mathrm{cal\,K^{-1}\,mol^{-1}}$, for this temperature range (Eq. (4)). Assuming linearity up to 60 °C, the intrinsic binding enthalpy at 60 °C, ΔHint (60 °C), was calculated as −32.9 ± 4.0 kcal/mol (Eq. (7)). Eqs. (5) and (6) describe ΔCP and ΔHint (60 °C), respectively, in terms of the polar and apolar components of ΔASA (the change in accessible surface area). Solving this set of equations and neglecting the impact of ΔASA_{OH} on ΔCP, yielded a calculated ΔASApolar of 1610 Å2 and ΔASApolar of 1480 $Å^2$. This ΔASAtotal of 3090 Å2 reflects a large protein-protein interface, according to [63].

Many organic osmolytes such as sucrose and glycerol show a net exclusion from protein interfaces as water molecules are drawn away. Then the depleted areas are destabilized by the osmotic pressure [61]. Subsequently, the burial of destabilized areas becomes increasingly favorable when more osmolyte is present in the vicinity of the protein. Consequently, if burial of interfacial areas takes place during ligand binding, then addition of an osmolyte could change the binding strength of the proteins and their ligands [62], in proportion to the osmolyte concentration. Therefore, we conducted experiments under different osmotic stress conditions by introducing varying concentrations of sucrose to the solvent (Fig. 4). The slope of the linear regression between the natural logarithm of the binding association constant (K_a) and the sucrose concentration is correlative to the number of water molecules (nW) exchanged between the complex and the bulk solvent during the interaction (Eq. (8)). Accordingly, n_W of this interaction was found to be −95.6.

3.2. FNR does not bind PSI* from C. reinhardtii

In contrast to PSI-LHCI, PSI* did not bind FNR under the same set of conditions (and even while using higher PSI* concentration). As can be viewed in Fig. 5, the heat signals from the titration were weak and invariant. FNR binding was related in the past to PsaE subunit of PSI [27,29], and PsaE levels were similar in both PSI-LHCI and PSI* particles [46]; however, this finding indicates that the presence of PsaE has a limited role if any in the binding of FNR to PSI.

4. Discussion

The current study showed that FNR binds PSI-LHCI with a stoichiometry of a single binding site per PSI in *C. reinhardtii*. Recently, the association of FNR with the thylakoid membrane and PSI in *C. reinhardtii* was shown to be impaired in the absence of PGR5 and/or PGRL1. It was proposed that these proteins contribute directly or indirectly to the recruitment of FNR to the thylakoid membrane *in vivo* [6]. In a different study, PGRL1 was co-purified with FNR and PSI from *C. reinhardtii* as part of the elusive cyclic electron flow super-complex, while PGR5 was not detected [18]. However, the *in vitro* association between the purified components described in this study was direct and did not involve PGR5 or PGRL1, as both of these proteins could not be detected in the purified PSI-LHCI particles by peptide MS [46].

The FNR:PSI-LHCI complexation is enthalpy driven (Fig. 1). The strong favorable (negative) enthalpy indicates the formation of optimal contacts between FNR and PSI (van der Waals interactions and hydrogen bonds) that surely overcome the penalty of polar groups desolvation enthalpy, which is the major contributor to the unfavorable binding enthalpy (positive) [64,65]. The entropy contribution mainly describes an interplay between two processes: (1) the favorable desolvation entropy, which arises from the burial of hydrophobic areas during binding and the resulting increase in the solvent entropy; and (2) the unfavorable conformational entropy change due to the loss of conformational degrees of freedom upon binding [64,66]. The latter process, which is ruling the entropy contribution in this interaction, implies large conformational changes (*e.g.* significant number of instances with immobilization of flexible peptides) and disorder-to-order transition in general during FNR:PSI-LHCI binding. An early study in spinach measured anisotropy changes of labeled FNR in reconstituted thylakoid membranes (*i.e.* membranes that were washed of FNR and incubated with the labeled enzyme) [8]; conformational changes were reported to occur in FNR upon binding, though only in the presence of added ferredoxin. The authors proposed that FNR binding to PSI, a large slowly rotating component of the thylakoid membrane, accounts

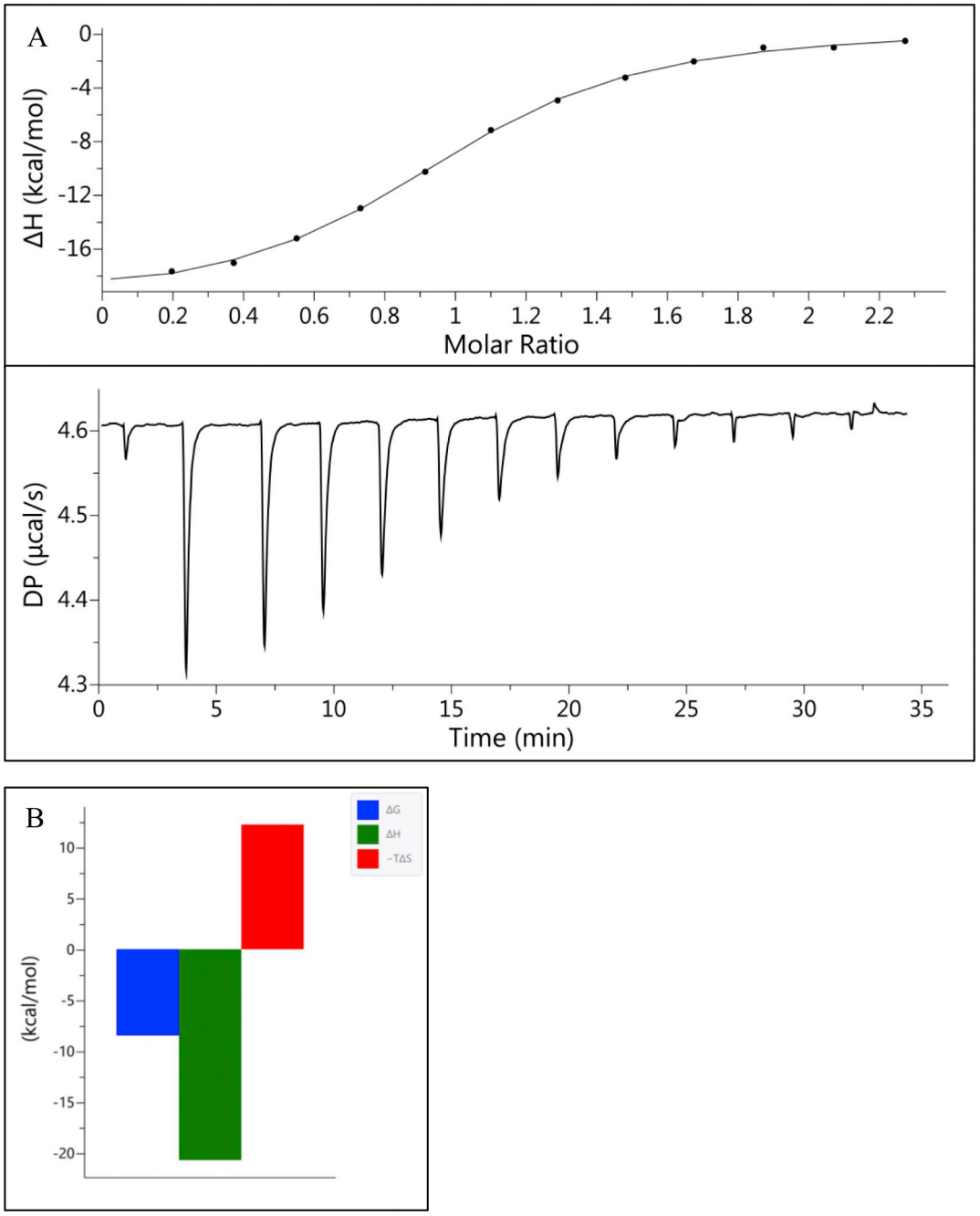

Fig. 1. Titration of PSI-LHCI with FNR. Panel A, titration of PSI-LHCI (6.4 µM in the ITC cell) with FNR (70 µM in the syringe) in 50 mM Hepes-KOH pH 7.5 buffer (0.05% DDM), at 25 °C. The raw heat changes (bottom pane) were subtracted with the mean value obtained from the titration of the blank buffer with FNR. The resulting sigmoid binding curve is shown at the top pane. Panel B, thermodynamic signature plot of FNR:PSI-LHCI binding. The large favorable enthalpy (green bar) is compensated by the unfavorable entropy component (red bar). $N = 0.94 \pm 0.02$; Kd = 780 ± 110 nM; $\Delta H = -20.7 \pm 0.8$ kcal/mol; $\Delta G = -8.3$ kcal/mol; $-T\Delta S = 12.4$ kcal/mol ($n = 4$).

for the observed slowing of the labeled FNR rotational diffusion [8].

4.1. Subunit like interaction between FNR and PSI-LHCI in C. reinhardtii

FNR binding to PSI in *C. reinhardtii* exhibits moderate affinity *in vitro*, with a Kd of 0.8 µM (Fig. 1) in slightly alkaline pH. However, the affinity in highly crowded conditions such as those that prevail in the stroma [67] would probably be higher. This is based on the titrations performed in various osmotic stress conditions, which showed a ~4.5-fold increased affinity in 1 M sucrose (Fig. 4). Molar concentrations of FNR in the stroma were estimated in the past as ~30 µM in maize leaves [68] and ~100 µM in cyanobacteria [67]. More recently in *Chlamydomonas*, FNR was measured as ~5.2 µmol g^{-1} Chl [69], which calculates to ~80 µM when using the 66 µL mg^{-1} Chl estimate for spinach chloroplast stromal volume [70]. These estimates present a picture in which FNR is constantly bound to PSI as if it was an additional subunit of the complex. Indeed, co-purified FNR:PSI were recently reported [18,33,34].

From a different perspective, in a proximal protein-protein binding system, a Kd of ~130 nM was measured for the binding of recombinant PsaD to a PsaD-less PSI from a thermophilic cyanobacterium [44]. It is interesting to note that PsaD is a genuine subunit of PSI and thus its affinity to PSI, measured at pH 7.0, was expected to be stronger than that of FNR.

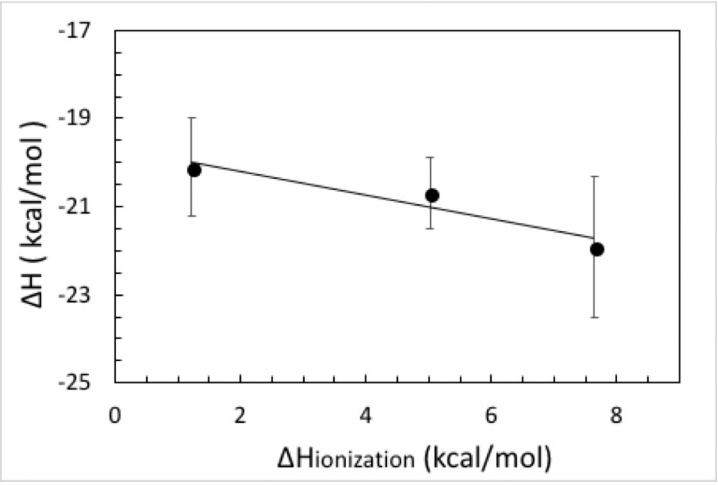

Fig. 2. The dependence of FNR:PSI-LHCI binding enthalpy (ΔH), on the buffer ionization enthalpy ($\Delta H_{ionization}$). Titrations were performed in 25 mM sodium phosphate (n = 3), 50 mM Hepes-KOH (n = 4) and 50 mM Tricine-NaOH (n = 4), pH 7.5, 0.05% DDM at 25 °C. The mean experimental ΔH values for each buffer were plotted against the specific buffer ionization enthalpy (1.22, 5.02 and 7.64 kcal/mol for phosphate, Hepes and Tricine, respectively). The line is a linear best fit of the data points according to Eq. (3) (nH+ = −0.27 ± 0.08, ΔH0 = −19.6 kcal/mol).

Following the demonstration of FNR binding to PSI-LHCI, additional experiments were performed to study the binding mechanism in *C. reinhardtii*. We found the possible contribution of buffer ionization to the binding enthalpy to be negligible (Fig. 2). However, that doesn't necessarily mean that FNR:PSI-LHCI binding is devoid of any ionization processes. Rather, proton release and proton uptake may offset each other [71].

Another interesting finding concerns the area of contact between FNR and PSI. The change in accessible surface area (ΔASA) was estimated from the measured heat capacity change, ΔCP (Fig. 3). Previously, several groups have shown that when a protein undergoes changes in its relations with its surrounding (*e.g.* folding/unfolding and ligand binding), there is a simple and linear connection between the enthalpy, ΔCP and ΔASA (Eqs. (5)–(6)) [43,72]. ASA is the size of the protein surface that is accessible to the solvent. In the context of binding, it also denotes the surface not buried within the protein-ligand interface [63]. Although this method was initially studied during the unfolding of proteins' native state [58,73], it was later applied for structural studies of protein-protein and protein-DNA interactions [57,63,74,75]. This direct relationship mainly reflects the desolvation of the interface rather than contributions to ΔCP from non-covalent interactions [57,58]. In this work, this estimation yielded a ΔASA of 3090 Å2, which reflects a large protein-protein interface according to a survey done by [63].

In a study by Lo Conte et al. (1999), 75 protein-protein complexes were analyzed and divided to sub-classes according to their interface size [63]; 27% of the complexes were classified in the large interface group (ΔASA of 2000–4700 Å2). Two features were identified as common in that group; their size resembles subunit interfaces in oligomeric proteins, and their formation is generally accompanied by major conformation changes [63]. As discussed above, FNR binds PSI-LHCI through a large interface that involves both conformational changes and a Kd value which is orders of magnitude lower than FNR concentration in the stroma. Therefore, it can be assumed that, in *C. reinhardtii*, FNR functions like a subunit of PSI-LHCI, in addition to its soluble sub-population and its participation in other thylakoid membrane complexes, such as the Cyt *b6f* and NDH.

Furthermore, we studied the role of water molecules in this large area of complexation between FNR and PSI. Water plays a mixed role in protein-protein affinity and interface stabilization. On the one hand, the entropic cost of immobilizing water molecules is high [65]; an interface deprived of water filling gaps will necessarily give a higher affinity. On the other hand, water molecules can also mediate the formation of hydrogen bonds, and the enthalpic gain in some cases may be greater than the entropic penalty [65]. In this work, binding experiments in different osmotic stress conditions revealed that the FNR:PSI-LHCI binding involves the release of ~96 water molecules to the solvent (Fig. 4).

It is interesting to compare the values of nW and ΔASA obtained in this study with those found using ITC for *Anabaena* Fd:FNR interaction by Martinez-Julvez et al. [43], for which a ΔASA of 1050 Å2 and a nW of −30 were reported. Notably, both values are about three times

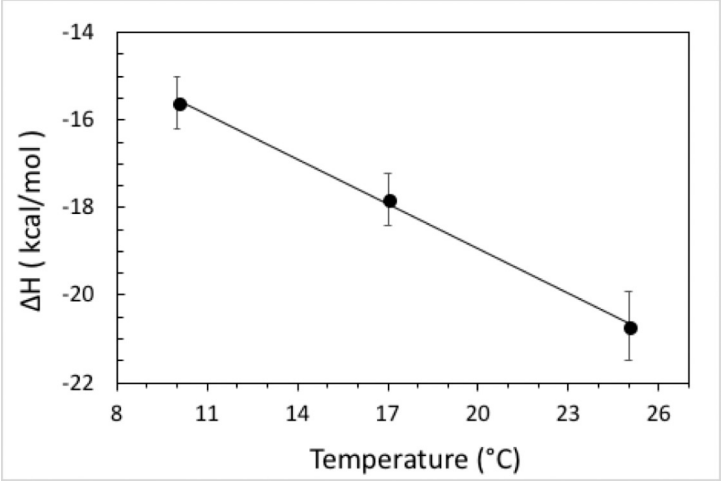

Fig. 3. The dependence of FNR:PSI-LHCI binding enthalpy, ΔH, on temperature. Titrations were performed in 50 mM Hepes-KOH, 0.05% DDM at 10 °C (n = 4), 17 °C (n = 3) and 25 °C (n = 5). The line is a linear fit according to Eq. (4), resulting in ΔCP of −340 ± 80 cal K^{-1} mol^{-1}.

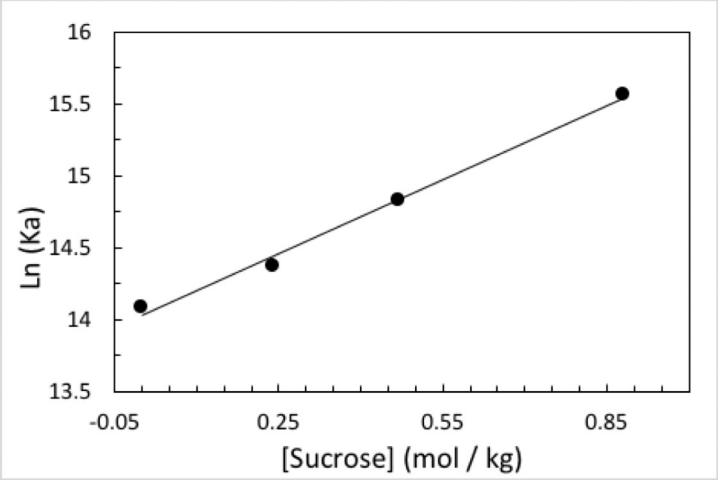

Fig. 4. The dependence of FNR:PSI-LHCI binding association constant (K_a) on solvent osmolality. Titrations were performed in 50 mM Hepes-KOH pH 7.5, 0.05% DDM supplemented with 0, 0.24, 0.47 (n = 2) or 0.88 mol/kg sucrose at 25 °C. The line is a best linear fit, yielding a slope of 1.72. The change in ln(K_a) as a function of the change in osmolality relates to nW through Eq. (8) (nW = −95.6).

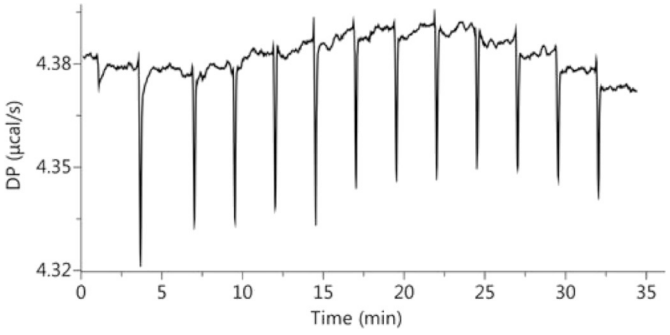

Fig. 5. Titration of PSI* with FNR. Titration of PSI* (6.4 µM in the ITC cell) with FNR (70 µM in the syringe) was performed in 50 mM Hepes-KOH pH 7.5 buffer (0.05% DDM), at 25 °C. The raw heat changes were invariant, indicating that no binding took place under this experimental setup.

smaller than those found for the FNR:PSI-LHCI system in this work. A ΔASA value of 1050 Å2 categorizes the Fd:FNR interaction in the group of small interfaces [63]. This group was suggested to represent the formation of short-lived, low stability protein complexes; likely, small conformational changes accompany the formation of this group [63]. Thus, for Fd:FNR, the small ΔASA together with a significant favorable entropy change (−TΔS = −3.1 kcal/mol; [43]) fits a somewhat rigid binding mechanism. Similarly, the binding of Fd and PSI, previously described in [46], supports a rigid binding mechanism as that interaction is also driven by a strong entropy change (−TΔS values between −10 and − 20 kcal/mol).

PSI*, the immature form, did not bind FNR, and this finding raises the question of which of the PSI-LHCI stroma-exposed subunits are involved in the interaction with the enzyme. Previously, the interaction of FNR with PSI through the PsaE subunit was shown using chemical cross-linking [27] and kinetic experiments [29] in barley and *Synechocystis*, respectively. Moreover, the positively charged N′ terminal of PsaE was speculated as being responsible for associating FNR in higher plants [31]. However, opposing results were also published [28,30]. In this work, PSI* was unable to bind FNR although PsaE levels are similar in both PSI-LHCI and PSI* preparations [46], which points to some other binding partner(s) besides PsaE. It is worth noting that Andersen et al. [27] reported that the 55 kDa cross-linking product was comprised of FNR and PsaE, but also low amounts of LHCI polypeptides, implying an additional connection of FNR to some LHCI polypeptide in barley.

As given by its name PSI-LHCI is comprised of the PSI core complex and the light harvesting complex I. The nine Lhca proteins in *C. reinhardtii* are organized in two layers, inner and outer, centered around the PsaF subunit. The configuration of individual LHCI subunits was recently shown by means of chemical cross-linking, immunoblotting and mass spectrometry [35,76]. The inner layer, from PsaG to PsaK, is comprised of Lhca1-Lhca8-Lhca7-Lhca3. It is possible that one or two of these inner layer subunits are associated with FNR in addition to PsaE. PsaF, -G and -K are likewise missing in the PSI* preparations [46], and therefore might also be candidates for FNR binding partners. PsaK position is at the end of the inner LHCI layer next to Lhca3 [35]. However, PsaK and Lhca3 access to PsaE is blocked when Fd is docked at the stromal ridge [76] (illustrated in Fig. 6A), making it unlikely for FNR to form simultaneous contact with both PsaE and either of the two subunits. Accordingly, the FNR docking site is expected to be at the stroma-facing plain of the PSI core, between PsaF and PsaG.

Fig. 6 presents a hypothetical illustration of the approximated FNR binding site (using PyMol software 2.0.7).Pea PSI crystallographic structure (*P. sativum*, PDB code 5L8R) [77] was used as an infrastructure, assuming the orientations of the four Lhca in the inner antennae belt of the pea are identical to *C. reinhardtii* PSI-LHCI [78]. The cyanobacterial Fd 3D representation (*Thermosynechococcus elongatus*, PDB code 5ZF0) was positioned in its active site according to [76]. FNR in complex with corn Fd (*Z. mays* root, PDB code 5H5J) [79] was superimposed over the Fd:PSI-LHCI model following few constraints: (1) it has to form contacts with PsaE; (2) it cannot block the Fd active site; (3) it has to form contacts with at least one of the inner belt Lhca proteins and also with PsaF/PsaG; (4) the binding interface should closely represent the large ΔASA estimation; (5) FNR orientation should enable functional activity while bound to PSI, *i.e.* Fd and NADP+ bindings should not be hindered. In order to satisfy the latter constraint, the opposite plain to the one used for Fd binding (PDB code 5H5J and 1GAQ; [79,80]) was assumed as the PSI binding interface of FNR. This also accords with the crystal structure of FNR in complex with Tic62-peptide from pea (PDB code 3MHP; [81]). Two FNR subunits were shown to bind the peptide in a back-to-back manner, in which Fd binding sites are accessible for both FNRs and thus activity is not affected by the interaction [81]. Taking all the above into consideration, the possible FNR binding sites are marked in Fig. 6A as three dashed black circles, where each circle roughly represents the dimensions of FNR's PSI-binding interface. A FNR:Fd 3D binding in one of the potential sites is shown in (Fig. 6C–D). We hypothesize that the actual site is found somewhere within the range marked by the circles, but further work is required to establish the validity of this proposed location. Although creating a crystal structure of the FNR:PSI-LHCI complex seems like a difficult task, recent progress in the field of cryo electron microscopy will hopefully shed some more light on the interactions in the photosynthetic membrane.

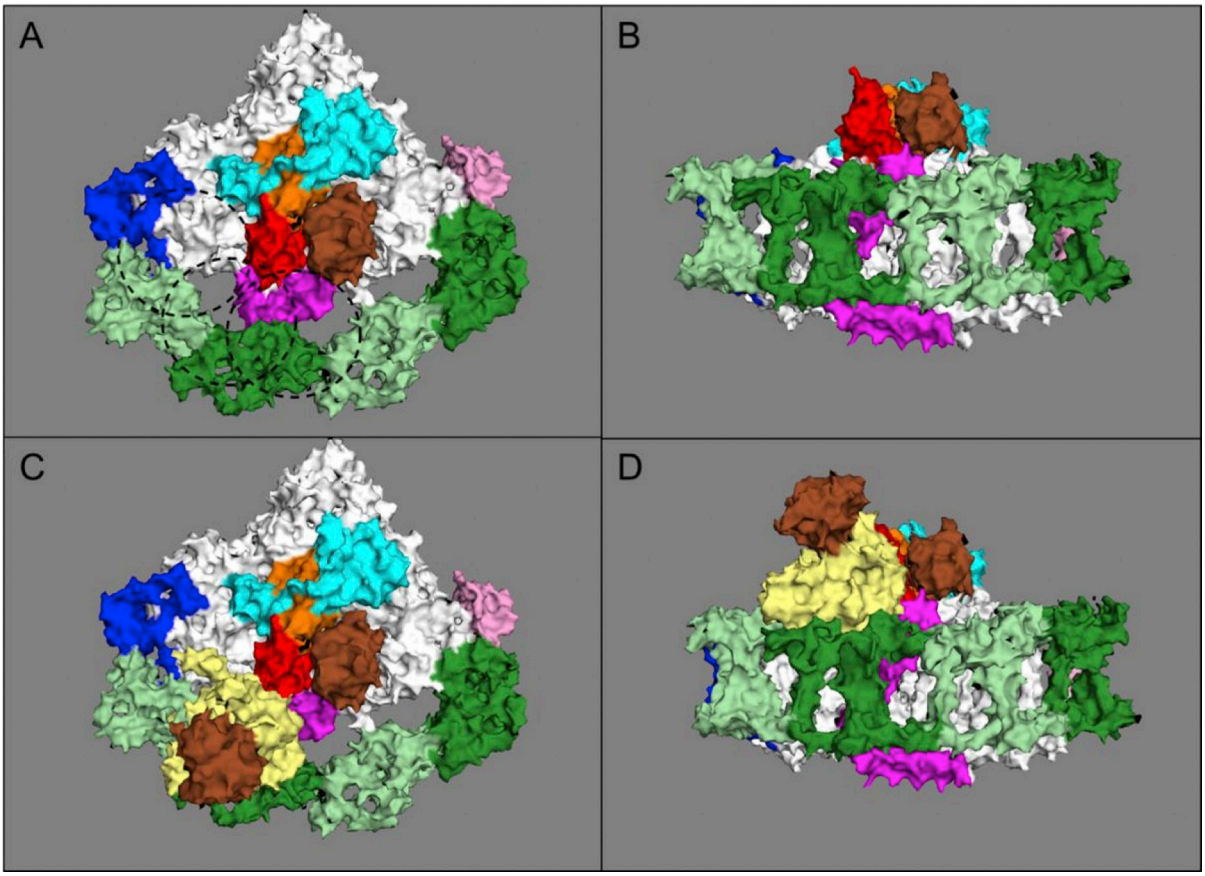

Fig. 6. A hypothetical structural superimposition of FNR over PSI-LHCI.
A model for the putative FNR binding site was illustrated, using PDB code 5L8R [77] as PSI-LHCI. Fd (derived from PDB code 5ZF0) was positioned in its binding site according to [76]. FNR in complex with Fd (PDB code 5H5J; [79]) was used to mark potential binding sites for FNR. *Panel A*, *Fd:PSI-LHCI from top view*. The three dashed black circles mark potential positions for FNR, where it may form contacts with PsaE, PsaB, at least one inner belt LHCI polypeptide and PsaF/PsaG. *Panel B*, *Fd:PSI-LHCI from side view*. *Panel C–D*, *superimposition of FNR:Fd in one Fd:PSI-LHCI potential binding site representation*. The structures are shown and were analyzed using PyMol software 2.0.7. The color code is as follows: core subunits (white); PsaC (orange); PsaD (cyan); PsaE (red); PsaF (magenta); PsaG (blue); PsaK (pink); Lhca1 and Lhca2 (light green); Lhca4 and Lhca3 (dark green); Fd (brown); FNR (yellow).

Transparency document

The Transparency document associated with this article can be found, in online version.

Acknowledgements

We would like to thank Prof. Adrian Velazquez-Campoy, from the University of Zaragoza (Spain) for the kind discussions, suggestions and sharing of his expertise in the field of ITC.

We would to thank Mr. Eyal Dafni for proofreading this MS.

The research was funded by Binational US-ISreael (BSF-NSF) 2016666 and by the Israel Science Foundation (ISF) 1646/16.

References

[1] W. Junge, N. Nelson, ATP synthase, Annu. Rev. Biochem. 84 (2015) 631–657.
[2] A.M. Terauchi, S.F. Lu, M. Zaffagnini, S. Tappa, M. Hirasawa, J.N. Tripathy, D.B. Knaff, P.J. Farmer, S.D. Lemaire, T. Hase, S.S. Merchant, Pattern of expression and substrate specificity of chloroplast ferredoxins from Chlamydomonas reinhardtii, J. Biol. Chem. 284 (2009) 25867–25878.
[3] T. Hase, P. Schurmann, D.B. Knaff, Govindjee, the interaction of ferredoxin with ferredoxin-dependent enzymes, in: J.H. Golbeck (Ed.), Springer, The Netherlands, Dordrecht, 2006, pp. 477–498.
[4] G. Hanke, P. Mulo, Plant type ferredoxins and ferredoxin-dependent metabolism, Plant Cell Environ. 36 (2013) 1071–1084.
[5] M. Winkler, A. Hemschemeier, J. Jacobs, S. Stripp, T. Happe, Multiple ferredoxin isoforms in Chlamydomonas reinhardtii - their role under stress conditions and biotechnological implications, Eur. J. Cell Biol. 89 (2010) 998–1004.
[6] L. Mosebach, C. Heilmann, R. Mutoh, P. Gäbelein, J. Steinbeck, T. Happe, T. Ikegami, G. Hanke, G. Kurisu, M. Hippler, Association of Ferredoxin:NADP + oxidoreductase with the photosynthetic apparatus modulates electron transfer in Chlamydomonas reinhardtii, Photosynth. Res. 134 (2017) 291–306.
[7] N. Carrillo, R.H. Vallejos, Interaction of ferredoxin-NADP oxidoreductase with the thylakoid membrane, Plant Physiol. 69 (1982) 210–213.
[8] R. Wagner, N. Carrillo, W. Junge, R.H. Vallejos, On the conformation of reconstituted ferredoxin:NADP + oxidoreductase in the thylakoid membrane. Studies via triplet lifetime and rotational diffusion with eosin isothiocyanate as label, Biochim. Biophys. Acta Bioenerg. 680 (1982) 317–330.
[9] N. Carrillo, R.H. Vallejos, The light-dependent modulation of photosynthetic electron transport, Trends Biochem. Sci. 8 (1983) 52–56.
[10] G. Forti, M. Bracale, Ferredoxin—ferredoxin NADP reductase interaction: catalytic differences between the soluble and thylakoid-bound complex, FEBS Lett. 166 (1984) 81–84.
[11] H. Zhang, J.P. Whitelegge, W.A. Cramer, Ferredoxin:NADP + oxidoreductase is a subunit of the chloroplast cytochrome b6fComplex, J. Biol. Chem. 276 (2001) 38159–38165.
[12] H.C. Matthijs, S.J. Coughlan, G. Hind, Removal of ferredoxin:NADP + oxidoreductase from thylakoid membranes, rebinding to depleted membranes, and identification of the binding site, J. Biol. Chem. 261 (1986) 12154–12158.
[13] M. Shin, H. Ishida, Y. Nozaki, A new protein factor, connectein, as a constituent of the large form of ferredoxin-NADP reductase, Plant Cell Physiol. 26 (1985) 559–563.
[14] S. Nakatani, M. Shin, The reconstituted NADP photoreducing system by rebinding of the large form of ferredoxin-NADP reductase to depleted thylakoid membranes, Arch. Biochem. Biophys. 291 (1991) 390–394.
[15] F.C. Soncini, R.H. Vallejos, The chloroplast reductase-binding protein is identical to the 16.5-kDa polypeptide described as a component of the oxygen-evolving complex, J. Biol. Chem. 264 (1989) 21112–21115.
[16] R.D. Clark, M.J. Hawkesford, S.J. Coughlan, J. Bennett, G. Hind, Association of ferredoxin-NADP + oxidoreductase with the chloroplast cytochrome b-f complex,

FEBS Lett. 174 (1984) 137–142.
[17] S. Coughlan, H.C. Matthijs, G. Hind, The ferredoxin-NADP+ oxidoreductase-binding protein is not the 17-kDa component of the cytochrome b/f complex, J. Biol. Chem. 260 (1985) 14891–14893.
[18] M. Iwai, K. Takizawa, R. Tokutsu, A. Okamuro, Y. Takahashi, J. Minagawa, Isolation of the elusive supercomplex that drives cyclic electron flow in photosynthesis, Nature 464 (2010) 1210–1213.
[19] H. Zhang, A. Primak, J. Cape, M.K. Bowman, D.M. Kramer, W.A. Cramer, Characterization of the high-spin heme x in the cytochrome b6f complex of oxygenic photosynthesis, Biochemistry 43 (2004) 16329–16336.
[20] W.A. Cramer, H. Zhang, Consequences of the structure of the cytochrome b6f complex for its charge transfer pathways, Biochim. Biophys. Acta 1757 (2006) 339–345.
[21] P. Mulo, Chloroplast-targeted ferredoxin-NADP+ oxidoreductase (FNR): Structure, function and location, Biochimica et Biophysica Acta (BBA) - Bioenergetics, 1807 (2011) 927–934.
[22] G. Guedeney, S. Corneille, S. Cuine, G. Peltier, Evidence for an association of ndh B, ndh J gene products and ferredoxin-NADP-reductase as components of a chloroplastic NAD(P)H dehydrogenase complex, FEBS Lett. 378 (1996) 277–280.
[23] R. Kouřil, O. Strouhal, L. Nosek, R. Lenobel, I. Chamrád, E.J. Boekema, M. Šebela, P. Ilík, Structural characterization of a plant photosystem I and NAD(P)H dehydrogenase supercomplex, Plant J. 77 (2014) 568–576.
[24] K.N. Yadav, D.A. Semchonok, L. Nosek, R. Kouril, G. Fucile, E.J. Boekema, L.A. Eichacker, Supercomplexes of plant photosystem I with cytochrome b6f, light-harvesting complex II and NDH, Biochim. Biophys. Acta Bioenerg. 1858 (2017) 12–20.
[25] J.P. Benz, A. Stengel, M. Lintala, Y.H. Lee, A. Weber, K. Philippar, I.L. Gügel, S. Kaieda, T. Ikegami, P. Mulo, J. Soll, B. Bölter, Arabidopsis Tic62 and ferredoxin-NADP(H) oxidoreductase form light-regulated complexes that are integrated into the chloroplast redox poise, Plant Cell 21 (2009) 3965–3983.
[26] S. Jurić, K. Hazler-Pilepić, A. Tomašić, H. Lepeduš, B. Jeličić, S. Puthiyaveetil, T. Bionda, L. Vojta, J.F. Allen, E. Schleiff, H. Fulgosi, Tethering of ferredoxin:NADP + oxidoreductase to thylakoid membranes is mediated by novel chloroplast protein TROL, Plant J. 60 (2009) 783–794.
[27] B. Andersen, H.V. Scheller, B.L. Moller, The PSI-E subunit of photosystem I binds ferredoxin:NADP+ oxidoreductase, FEBS Lett. 311 (1992) 169–173.
[28] N. Weber, H. Strotmann, On the function of subunit PsaE in chloroplast photosystem I, Biochim. Biophys. Acta 1143 (1993) 204–210.
[29] J.J. van Thor, T.H. Geerlings, H.C. Matthijs, K.J. Hellingwerf, Kinetic evidence for the PsaE-dependent transient ternary complex photosystem I/ferredoxin/ferredoxin:NADP(+) reductase in a cyanobacterium, Biochemistry 38 (1999) 12735–12746.
[30] N. Cassan, B. Lagoutte, P. Setif, Ferredoxin-NADP+ reductase, Kinetics of electron transfer, transient intermediates, and catalytic activities studied by flash-absorption spectroscopy with isolated photosystem I and ferredoxin, The Journal of biological chemistry 280 (2005) 25960–25972.
[31] C.J. Falzone, Y.H. Kao, J. Zhao, D.A. Bryant, J.T. Lecomte, Three-dimensional solution structure of PsaE from the cyanobacterium Synechococcus sp. strain PCC 7002, a photosystem I protein that shows structural homology with SH3 domains, Biochemistry, 33 (1994) 6052–6062.
[32] H. Takahashi, S. Clowez, F.A. Wollman, O. Vallon, F. Rappaport, Cyclic electron flow is redox-controlled but independent of state transition, Nat. Commun. 4 (2013) 1954.
[33] H. Takahashi, A. Okamuro, J. Minagawa, Y. Takahashi, Biochemical characterization of photosystem I-associated light-harvesting complexes I and II isolated from state 2 cells of Chlamydomonas reinhardtii, Plant Cell Physiol. 55 (2014) 1437–1449.
[34] S.V. Bergner, M. Scholz, K. Trompelt, J. Barth, P. Gabelein, J. Steinbeck, H. Xue, S. Clowez, G. Fucile, M. Goldschmidt-Clermont, C. Fufezan, M. Hippler, STATE TRANSITION7-dependent phosphorylation is modulated by changing environmental conditions, and its absence triggers remodeling of photosynthetic protein complexes, Plant Physiol. 168 (2015) 615–634.
[35] S.I. Ozawa, T. Bald, T. Onishi, H. Xue, T. Matsumura, R. Kubo, H. Takahashi, M. Hippler, Y. Takahashi, Configuration of ten light-harvesting chlorophyll a/b complex I subunits in Chlamydomonas reinhardtii photosystem I, Plant Physiol. 178 (2018) 583–595.
[36] H. Fernando, C. Chin, J. Rosgen, K. Rajarathnam, Dimer dissociation is essential for interleukin-8 (IL-8) binding to CXCR1 receptor, J. Biol. Chem. 279 (2004) 36175–36178.
[37] L. Piubelli, G. Zanetti, H.R. Bosshard, Recombinant wild-type and mutant complexes of ferredoxin and ferredoxin:NADP+ reductase studied by isothermal titration calorimetry, Biol. Chem. 378 (1997) 715–718.
[38] S. Vega, O. Abian, A. Velazquez-Campoy, On the link between conformational changes, ligand binding and heat capacity, Biochim. Biophys. Acta 1860 (2016) 868–878.
[39] V. Linkuviene, G. Krainer, W.Y. Chen, D. Matulis, Isothermal titration calorimetry for drug design: precision of the enthalpy and binding constant measurements and comparison of the instruments, Anal. Biochem. 515 (2016) 61–64.
[40] K. Rajarathnam, J. Rosgen, Isothermal titration calorimetry of membrane proteins - progress and challenges, Biochim. Biophys. Acta 1838 (2014) 69–77.
[41] K. Zimmermann, M. Heck, J. Frank, J. Kern, I. Vass, A. Zouni, Herbicide binding and thermal stability of photosystem II isolated from Thermosynechococcus elongatus, Biochim. Biophys. Acta 1757 (2006) 106–114.
[42] I. Jelesarov, H.R. Bosshard, Thermodynamics of ferredoxin binding to ferredoxin:NADP+ reductase and the role of water at the complex interface, Biochemistry-Us 33 (1994) 13321–13328.
[43] M. Martinez-Julvez, M. Medina, A. Velazquez-Campoy, Binding thermodynamics of ferredoxin:NADP+ reductase: two different protein substrates and one energetics, Biophys. J. 96 (2009) 4966–4975.
[44] P. Jin, J. Sun, P.R. Chitnis, Structural features and assembly of the soluble overexpressed PsaD subunit of photosystem I, Biochim. Biophys. Acta 1410 (1999) 7–18.
[45] V. Pandini, A. Aliverti, G. Zanetti, Interaction of the soluble recombinant PsaD subunit of spinach photosystem I with ferredoxin I, Biochemistry-Us 38 (1999) 10707–10713.
[46] P. Marco, M. Kozuleva, H. Eilenberg, Y. Mazor, P. Gimeson, A. Kanygin, K. Redding, I. Weiner, I. Yacoby, Binding of ferredoxin to algal photosystem I involves a single binding site and is composed of two thermodynamically distinct events, Biochim. Biophys. Acta 1859 (2018) 234–243.
[47] G. Wittenberg, S. Jarvi, M. Hojka, S.Z. Toth, E.H. Meyer, E.M. Aro, M.A. Schottler, R. Bock, Identification and characterization of a stable intermediate in photosystem I assembly in tobacco, Plant J. 90 (2017) 478–490.
[48] N. Fischer, P. Setif, J.D. Rochaix, Targeted mutations in the psaC gene of Chlamydomonas reinhardtii: preferential reduction of FB at low temperature is not accompanied by altered electron flow from photosystem I to ferredoxin, Biochemistry 36 (1997) 93–102.
[49] N. Fischer, P. Setif, J.D. Rochaix, Site-directed mutagenesis of the PsaC subunit of photosystem I. F(b) is the cluster interacting with soluble ferredoxin, J. Biol. Chem. 274 (1999) 23333–23340.
[50] P. Setif, Ferredoxin and flavodoxin reduction by photosystem I, Biochim. Biophys. Acta 1507 (2001) 161–179.
[51] M. Shin, [40] ferredoxin-NADP reductase from spinach, Methods Enzymol. 23 (1971) 440–447.
[52] G. Gulis, K.V. Narasimhulu, L.N. Fox, K.E. Redding, Purification of His6-tagged photosystem I from Chlamydomonas reinhardtii, Photosynth. Res. 96 (2008) 51–60.
[53] R.J. Porra, The chequered history of the development and use of simultaneous equations for the accurate determination of chlorophylls a and b, Photosynth. Res. 73 (2002) 149–156.
[54] B. Drop, M. Webber-Birungi, F. Fusetti, R. Kouril, K.E. Redding, E.J. Boekema, R. Croce, Photosystem I of Chlamydomonas reinhardtii contains nine light-harvesting complexes (Lhca) located on one side of the core, J. Biol. Chem. 286 (2011) 44878–44887.
[55] H. Witt, E. Bordignon, D. Carbonera, J.P. Dekker, N. Karapetyan, C. Teutloff, A. Webber, W. Lubitz, E. Schlodder, Species-specific differences of the spectroscopic properties of P700: analysis of the influence of non-conserved amino acid residues by site-directed mutagenesis of photosystem I from Chlamydomonas reinhardtii, J. Biol. Chem. 278 (2003) 46760–46771.
[56] H. Fukada, K. Takahashi, Enthalpy and heat capacity changes for the proton dissociation of various buffer components in 0.1 M potassium chloride, Proteins 33 (1998) 159–166.
[57] J. Gomez, E. Freire, Thermodynamic mapping of the inhibitor site of the aspartic protease Endothiapepsin, J. Mol. Biol. 252 (1995) 337–350.
[58] J. Gomez, V.J. Hilser, D. Xie, E. Freire, The heat capacity of proteins, Proteins 22 (1995) 404–412.
[59] D. Xie, E. Freire, Molecular-Basis of Cooperativity in Protein-Folding. 5. Thermodynamic and Structural Conditions for the Stabilization of Compact Denatured States, Proteins, 19 (1994) 291–301.
[60] S. Bergqvist, M.A. Williams, R. O'Brien, J.E. Ladbury, Heat capacity effects of water molecules and ions at a protein-DNA interface, J. Mol. Biol. 336 (2004) 829–842.
[61] M. Auton, D.W. Bolen, Additive transfer free energies of the peptide backbone unit that are independent of the model compound and the choice of concentration scale, Biochemistry 43 (2004) 1329–1342.
[62] V.A. Parsegian, R.P. Rand, D.C. Rau, Macromolecules and water: probing with osmotic stress, Methods Enzymol. 259 (1995) 43–94.
[63] L. Lo Conte, C. Chothia, J. Janin, The atomic structure of protein-protein recognition sites, J. Mol. Biol. 285 (1999) 2177–2198.
[64] E. Freire, Do enthalpy and entropy distinguish first in class from best in class? Drug Discov. Today 13 (2008) 869–874.
[65] J.E. Ladbury, Just add water! The effect of water on the specificity of protein-ligand binding sites and its potential application to drug design, Chem. Biol. 3 (1996) 973–980.
[66] H. Ohtaka, E. Freire, Adaptive inhibitors of the HIV-1 protease, Prog. Biophys. Mol. Biol. 88 (2005) 193–208.
[67] G. Moal, B. Lagoutte, Photo-induced electron transfer from photosystem I to NADP+: characterization and tentative simulation of the in vivo environment, Biochim. Biophys. Acta Bioenerg. 1817 (2012) 1635–1645.
[68] S. Okutani, G.T. Hanke, Y. Satomi, T. Takao, G. Kurisu, A. Suzuki, T. Hase, Three maize leaf ferredoxin:NADPH oxidoreductases vary in subchloroplast location, expression, and interaction with ferredoxin, Plant Physiol. 139 (2005) 1451–1459.
[69] D. Nikolova, C. Heilmann, S. Hawat, P. Gäbelein, M. Hippler, Absolute quantification of selected photosynthetic electron transfer proteins in Chlamydomonas reinhardtii in the presence and absence of oxygen, Photosynth. Res. 137 (2018) 281–293.
[70] H. Winter, D.G. Robinson, H.W. Heldt, Subcellular volumes and metabolite concentrations in spinach leaves, Planta 193 (1994) 530–535.
[71] B. Baum, L. Muley, A. Heine, M. Smolinski, D. Hangauer, G. Klebe, Think twice: understanding the high potency of Bis(phenyl)methane inhibitors of thrombin, J. Mol. Biol. 391 (2009) 552–564.
[72] E. Freire, Thermodynamics of protein folding and molecular recognition, Pure Appl. Chem. 69 (1997) 2253–2261.
[73] J.R. Livingstone, R.S. Spolar, M.T. Record, Contribution to the thermodynamics of protein folding from the reduction in water-accessible nonpolar surface-area,

Biochemistry 30 (1991) 4237–4244.
[74] V.J. Hilser, J. Gomez, E. Freire, Enthalpy change in protein folding and binding: refinement of parameters for structure-based calculations, Proteins Struct. Funct. Genet. 26 (1996) 123–133.
[75] R.S. Spolar, M.T. Record, Coupling of local folding to site-specific binding of proteins to DNA, Science 263 (1994) 777–784.
[76] H. Kubota-Kawai, R. Mutoh, K. Shinmura, P. Setif, M.M. Nowaczyk, M. Rogner, T. Ikegami, H. Tanaka, G. Kurisu, X-ray structure of an asymmetrical trimeric ferredoxin-photosystem I complex, Nat. Plants 4 (2018) 218–224.
[77] Y. Mazor, A. Borovikova, N. Nelson, The structure of plant photosystem I supercomplex at 2.8A resolution, Nat. Plants 3 (2017) 17014.
[78] X. Su, J. Ma, X. Pan, X. Zhao, W. Chang, Z. Liu, X. Zhang, M. Li, Antenna arrangement and energy transfer pathways of a green algal photosystem-I–LHCI supercomplex, Nat. Plants 5 (2019) 273–281.
[79] F. Shinohara, G. Kurisu, G. Hanke, C. Bowsher, T. Hase, Y. Kimata-Ariga, Structural basis for the isotype-specific interactions of ferredoxin and ferredoxin: NADP(+) oxidoreductase: an evolutionary switch between photosynthetic and heterotrophic assimilation, Photosynth. Res. 134 (2017) 281–289.
[80] G. Kurisu, M. Kusunoki, E. Katoh, T. Yamazaki, K. Teshima, Y. Onda, Y. Kimata-Ariga, T. Hase, Structure of the electron transfer complex between ferredoxin and ferredoxin-NADP+ reductase, Nat. Struct. Biol. 8 (2001) 117–121.
[81] F. Alte, A. Stengel, J.P. Benz, E. Petersen, J. Soll, M. Groll, B. Bölter, Ferredoxin:NADPH oxidoreductase is recruited to thylakoids by binding to a polyproline type II helix in a pH-dependent manner, Proc. Natl. Acad. Sci. 107 (2010) 19260–19265.